Himalayan Geology, Vol. 46 (2), 2025, pp. 184-195, Printed in India

Stress pattern analysis and its tectonic implications in the Eastern Himalayan Syntaxis: A special emphasis to the Siang Valley, Arunachal Pradesh, Northeast India

ASHISH PAL[1,2], DILIP KUMAR YADAV[1,*], DEBONIL BARUAH[1], ABHISHEK KUMAR GUPTA[1], H.C. NAINWAL[2], PARAKH SAHU[1]

[1]*Wadia Institute of Himalayan Geology, Dehradun-248001, India*
[2]*Hemvati Nandan Bahuguna Garhwal University, Srinagar Garhwal-246174, India*
**Email (Corresponding author): dilipky@yahoo.com*

Abstract: The Siang Valley of northeast Himalaya is one of the most seismotectonically active area that lies within the Eastern Himalayan Syntaxis (EHS). In this study the Focal Mechanism Solutions (FMSs) are determined and estimated FMSs are used to understand the existing stress field in the region. The depth distribution of seismicity ranges up to a focal depth of 60 kilometers, with a higher concentration in the upper crustal part. We estimated 18 FMSs using P-wave first motion for the events having a magnitude (M_L) ranging from 3.5 to 5.4, showing normal, thrust and a combination of strike-slip mechanism which follows the major tectonic feature/faults in the region. From the analysis of stress inversion, it is observed that the direction of the highest compression (P) axis is SSE, indicating the presence of a radial compressional stress regime in the western part of Siang Valley. In the eastern part of Siang Valley, a predominant transtension stress regime is observed and P axis is oriented in the SSW direction. The Siang Valley and adjoining region, the estimated maximum principal stress ($\sigma 1$) shows a trend towards the SSW direction. The stress regime index (R') indicates a strike slip with reverse faulting occurring in this region. The FMSs and stress tensor outlined in our study provide valuable insights for developing a more comprehensive understanding of the seismotectonic implications in this area. This information is beneficial for evaluating seismic hazards and related geodynamic activities.

Keywords: Focal mechanism solutions, Stress tensor, Siang Valley, Eastern Himalayan Syntaxis

INTRODUCTION

The Eastern Himalayan Syntaxis (EHS) of Arunachal Pradesh, NE India, is one of the most seismotectonically dynamic region. In Northeast India, a convergence was observed among three significant tectonic plates, namely Indian, Eurasian, and Burmese. This phenomenon encompasses the presence of two primary mountain ranges; in the north are the Himalayas, and in the southeast are the Indo-Burmese Ranges, accompanied by a significant intraplate area in Northeast India. There is an agreement on the presence of north-south compression triggered by the collision of plates between India and Eurasia. The specifics regarding the directional variations in compression and the nature of alignments of seismotectonic stress patterns, still need to be more adequately understood. The absence of clarity is notably evident in the Assam syntaxis region, where the meeting point of the two primary mountain ranges occurs near the coordinates 28ºN and 96ºE. Previous studies have emphasized the importance of continental collision in this scenario (Molnar & Tapponnier 1975; Mitchell 1981; Curray *et al.* 1982; Tapponnier *et al.* 1982, 1986). The Himalayan range represents the largest orogenic belt globally, where one continental crust subducts beneath another continental crust. This geological phenomenon has been extensively studied (Le Fort 1975; Nandy 2001; Zhao *et al.* 1993; Mitra *et al*. 2005). The amalgamating structures constituting a complex geo-tectonic framework (Curray *et al.* 1982) exert pressure on the northeastern sector of the Indian plate, resulting in deformation (Chen and Molnar 1990; Kayal 1991; Bilham & England 2001). From a broader perspective, the Arunachal Himalaya encompasses the furthest eastern section of the Himalaya, situated between longitudes 91º30 E and 96ºE, encompassing the EHS. The Indian plate is gently dipping to the north beneath the Himalayas (Zhao *et al.* 1993; Mitra *et al.* 2005). The northeastern syntaxis of the Himalaya delineates the region in which the Himalayan arc undergoes a significant southward trend, situated proximate to the eastern boundary shared by India and China. Seismic activity is notably influenced by the intraplate deformation within northeastern India and the eastern Himalayan syntaxis caused by the collision of India with Eurasia and the subduction of India beneath Burma. Earlier studies (Bilham 2006; Thingbaijam *et al.* 2008; Kayal *et al.* 2006) have documented that Namche Barwa massif (NB), a prominent dome-shaped formation marking the termination of the Himalayan Arc in the east, exhibits substantial seismicity (Khattri *et al.* 1983). This region is seismically active (Das Gupta & Nandy 1982; Gupta *et al*. 1984; Kayal & De Reena 1991; Baruah *et al.* 1997; Kayal 1998; Rajendran *et al.* 2004; Bilham 2006; Kayal *et al.* 2006; Thingbaijam *et al.* 2008), with the remarkable exception of the Assam Gap (Khattri *et al.* 1983).

EHS and its surrounding area have encountered two big seismic events namely, 1947 Ms 7.7 Lang earthquake and 1950 Ms 8.6 Zayu earthquake along with several minor tremors, predominantly clustered in the northeastern region which were mainly concentrated in the north eastern part of the EHS. In contrast, fewer earthquakes have occurred in the western part of the EHS and in the Namche Barwa (NB) area (Yang *et al.* 2018). The spatial distribution and characteristics of the shallow and intermediate earthquakes suggest subduction and collision of the crust in the upper part of the Himalayan arcuate range (Priestley *et al*. 2008). Therefore, studying of these earthquake will provide more insights of seismicity around EHS. Seismicity is usually concentrated in a narrow zone of about 50-70 kilometers wide, traversing along the Main Central Thrust (MCT) in EHS, which is one of the major fault systems in the Himalayas. The other two are the Main Boundary Thrust (MBT) and the Himalayan Frontal

Thrust (HFT) in this region (Ni & Barazangi 1984). The geometry and friction of the Main Himalayan Thrust (MHT) play a significant role in controlling seismic ruptures and stress interactions. The seismic activity in the Siang Valley is notable, with earthquakes manifesting in various zones at depths ranging from 5 to 45 km (Rai *et al.* 2024). The determination of seismotectonic stress regimes within a region is performed through the analysis of FMSs of earthquakes. This analysis provides new perspectives on the active tectonics of the region and facilitates the evaluation of geodynamic implications. Typically, the focal mechanism solution pertains to the fault orientation, the seismic slip with respect to the plate motion and stress release patterns. Rastogi *et al.* (1973) ascertained 11 FMSs for earthquakes that occurred in the Assam-Myanmar region by utilizing P-wave first-motion direction data. Their findings indicated that the primary modes of deformation observed in the region are associated with thrust faulting. Chandra (1978) calculated a total of eighteen FMSs for the seismic events in the Himalayan region by employing P-wave first motion data. The findings revealed a predominant thrust faulting pattern in the northeast region of India. Pal *et al.* (2024a) studied the source parameter and seismotectonic analysis in the Siang Valley region of northeastern Himalaya. The investigation into the focal mechanism solution by Hazarika *et al.* (2022) and the stress inversion study by Kamra *et al.* (2023) was executed in the northeastern sector of the eastern Himalayan Syntaxis.

In our present study, using the recently acquired seismic data, i.e. more data compared with previous studies, evaluation of FMSs using P- wave first polarity method with the depth section across the Siang window and stress tensor inversion has been applied using focal mechanisms of events that occurred in the Siang Valley, NE Himalayas. We focused on investigating the trend of the primary stress axes to comprehend the local-regional stress field in the region which are divided into two sub-region.

GEOLOGY AND TECTONICS

Siang Valley is located in the eastern part of the Himalayas, where the Himalayan arc bends sharply southward. The tectonic setting of Siang Valley is complex and involves different tectonic units and fault systems. A large antiform structure called the Siang antiform, dominates the Siang Valley, which exposes the Lesser Himalayan Crystalline Sequence (LHCS) (Fig. 1) The LHCS is a representation of a metamorphic belt consisting of gneisses, schists, quartzites and marbles, situated within the eastern flank of the Siang antiform (Gururajan & Choudhuri 2003; Misra 2009); the LHCS's boundaries are delineated by Trans-Himalayan tectonic units, specifically the Tidding suture zone and the Lohit plutonic complex (LPC). The centre of the Siang antiform is characterized by sedimentary rocks of the Mesozoic era (Singh 1993). In the Siyom Valley, which is a tributary of the Siang River, the LHCS is structurally detached from the Lesser Himalayan Sequence (LHS) by the Main Central Thrust-I (MCT-I) at a lower structural level; nevertheless, it is in juxtaposition with the Higher Himalayan Crystalline Sequence (HHCS) along Main Central Thrust-II (MCT-II) at a higher structural level. MCT-I and MCT-II are prominent thrust faults responsible for accommodating crustal shortening and thickening in the Himalayan region. The MCT and MBT depict the primary tectonic characteristics observed in the Eastern Himalayan region. The Main Central Thrust (MCT) has been identified as a significant intracontinental ductile shear zone, which is linked to an inverted metamorphic zone that is thought to have formed since the mid-Tertiary period, shows minor recent movements as well (Valdiya 1980). Acting as a demarcation line, the MCT divides two distinctive geological terrains - the Lesser Himalaya situated to the south and in the north higher Himalayan Crystallines. The primary geological division differentiates the lesser and sub-Himalayan areas by the Main Boundary Thrust (MBT), acknowledged for its continuous high seismic activity leading to devastating earthquakes. This prominent thrust belt emerged during the Pliocene epoch and remained dynamic throughout the Pleistocene era (Valdiya 1980). The Assam syntaxis zone is situated within the easternmost part of the Himalayas, representing a significant tectonic region where the convergence of the Himalayan arc, Burmese arc, and Mishmi block occurs, featuring thrust trends in the NW-SE direction as evidenced by the Lohit and Mishmi thrusts (Fig. 1). It is worth noting that this particular zone was the focal point of the major earthquake of 1950 as documented (Poddar 1950).

METHODOLOGY

Seismic Network and Data

The Wadia Institute of Himalayan Geology (WIHG) Dehradun has installed a network comprising 8 broad-band Seismic (BBS) stations in the Siang Valley, Northeast India, with the primary objective of investigating the Seismotectonic attributes of the region. The initiation of the seismic stations' operations occurred in December 2018, as documented by Yadav *et al.* (2021). Positioned on top of Granitoids rocks, the Gelling (GLNG) seismic station is the most northerly station, while the Jengging (JNGG) station is located on the gneissic rocks of the Lesser Himalayas. The Mariyang (MRNG) and Yingkiong (YINK) seismic stations are positioned on the Yingkiong formation (Acharyya & Saha 2013). The Along (ALON) station is located on the sequences of the Lesser Himalayas, whereas the Padu (PADU) and Boleng (BLNG) stations are found on the Miri Quartzite. The Pasighat (PASI) seismic station, the station furthest to the south, is situated on the alluvial sediments of the Brahmaputra River Basin. The BBS stations are furnished with a three-component Trillium Compact-120 sensor and Centaur digitizer. The instrument is configured with a compact flash memory card intended for the continuous recording of data of 100 samples per second (SPS). A sensitivity of 1500 V/m/s is demonstrated by the digitizer. These seismic stations operate independently and are furnished with GPS receivers to ensure accurate time synchronization.

The SEISAN analysis software by Havskov & Ottemoller (1999) was utilized to examine and distinguish the P and S-phases for the purpose of determining the hypocentral

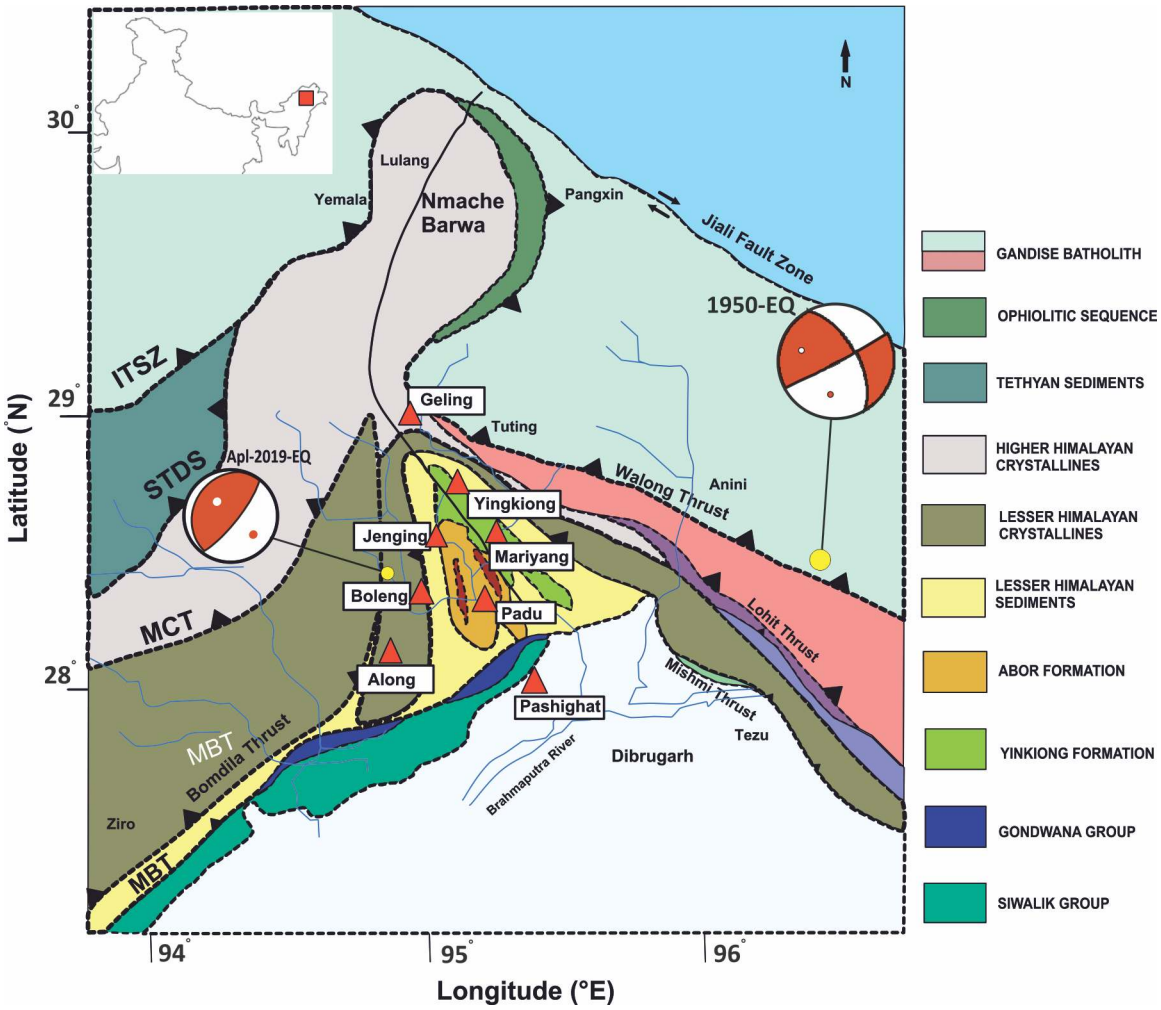


Fig. 1. Geology and Tectonic map of the Siang Valley in the Eastern Himalayan Syntaxis of the northeast Himalaya (modified after Yadav *et al.* 2021). The installation of broad band Seismic stations by WIHG is denoted by red triangles on the map. Various significant tectonic features such as the MBT, MCT, STDS, ITSZ, Lohit Thrust, Walong Thrust, and Mishmi Thrust can be identified in the region. The rivers in the area are represented by blue lines.

parameters of the earthquake. The hypocentral parameters are computed using the HYPO71 software, which was created by Lee & Lahr (1975). For the computational studies of seismic events, a five-layer velocity model (Table 1) introduced by Raoof *et al.* (2017) with Vp/Vs ratio of 1.74 is employed. The seismic events are identified, processed, and relocated to produce a Seismological catalogue of Siang Valley within the geographical coordinates of 27.75°- 29.25°N Latitude and 94.5°-96°E Longitude (Fig. 2). The uncertainties in epicenter locations range approximately ±5 km, with the Root Mean Square (RMS) value varying from 0.2 to 0.5 seconds.

Focal Mechanism Solution

FMSs are determined from the P wave first motion polarity using the FOCMEC application, as elaborated by Snoke *et al.* (1984). The package contains programs for determining and displaying double-couple earthquake focal mechanism. Input data are polarities (P, SV, SH) and/or amplitude ratios (SV/P, SH/P, SV/SH). The application performs an efficient, systematic search of the focal sphere. Application have been made to finding best constrained fault plane solutions for suits of earthquakes recorded at local to regional distances and using recorded polarities and relative amplitudes to produce waveforms synthetics (Snoke 2003). Employing the lower hemisphere equal area projection, the P and T axes correspondingly represent the directions of compression and tension. Within this framework, the compressional quadrant is illustrated by the shaded region on the focal sphere, while the dilatational quadrant remains unshaded. The determination of fault geometry by employing P-wave first motion data using FMS presents a direct approach, hinging on the polarity

Table 1. *1D velocity model of northeast India used for the present study (Raoof et al. 2017).*

Depth to the bottom layer	Vp(km/s)	Vs(km/s)
0	5.57	3.18
5	5.65	3.22
10	5.78	3.30
20	6.25	3.57
30	6.89	3.93
40	7.91	4.52
50	8.30	4.74

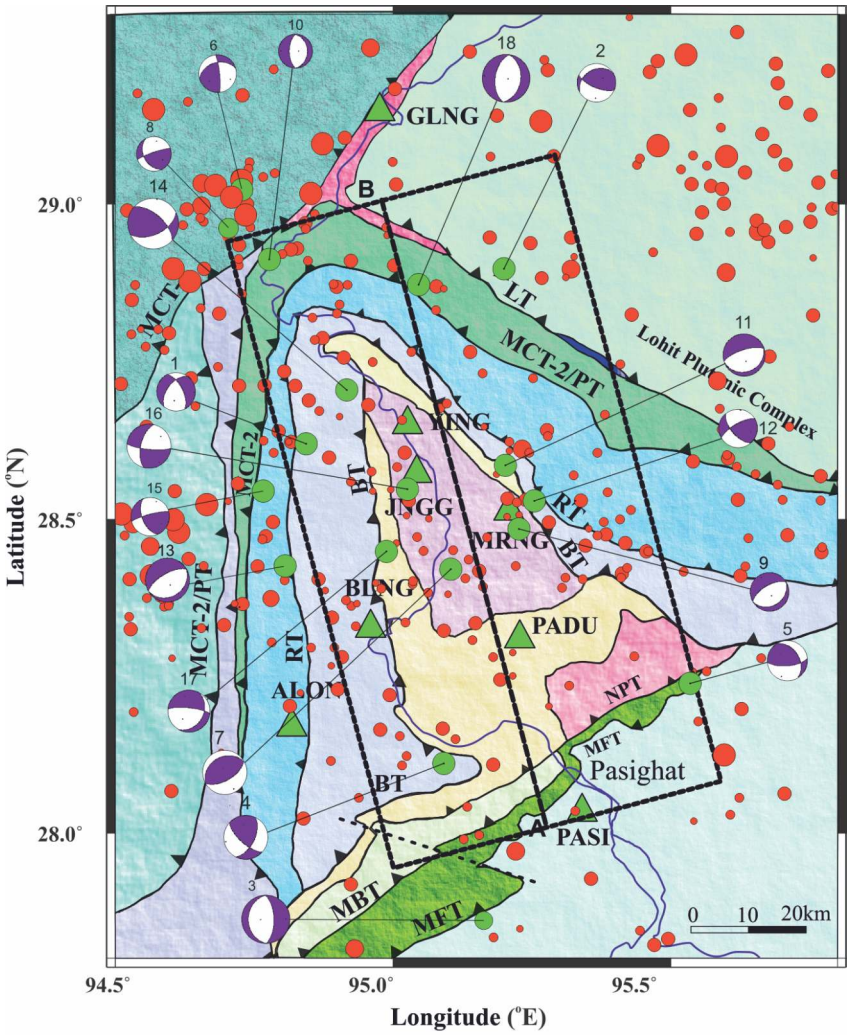


Fig. 2a. Plot depicting seismicity in and around Siang window and Focal Mechanism Solutions of selected events. Depth cross-section along A-B. Green triangles are BBS station. Varying red dots are corresponding size of earthquake events and green dots are earthquake events used for focal mechanism solutions (beach balls). The major tectonic characteristics depicted on the map include the North Pasighat Thrust (NPT), Main Frontal Thrust (MFT), Main Boundry Thrust (MBT), Main Central Thrust (MCT), Bomdo Thrust (BT), Ramgarh Thrust (RT) and Lohit Thrust (LT).

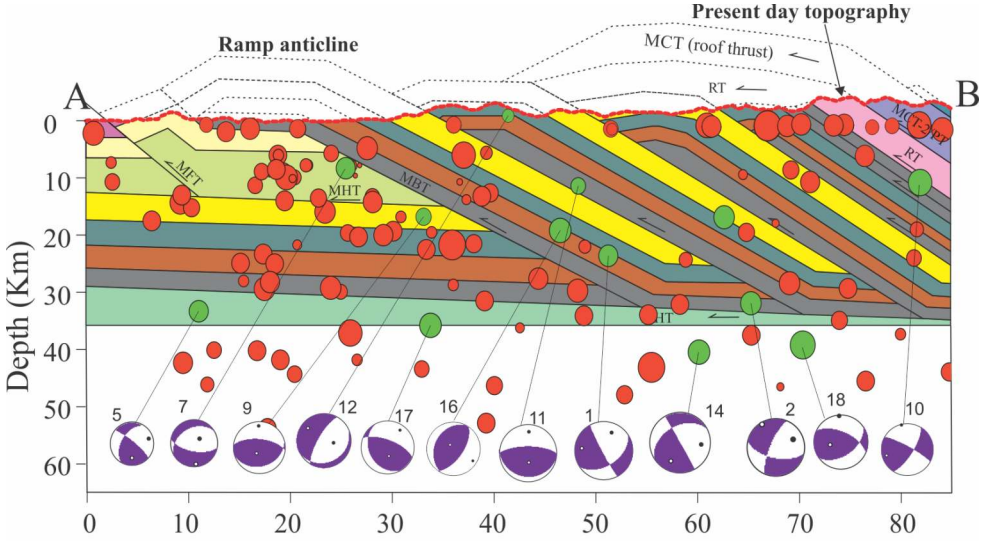


Fig. 2b. Plot (modified after Salvi *et al.* 2021) depicting Depth projected FMSs along section line A-B, highlighting the seismicity with respective depth. Tectonic features are Main Frontal Thrust (MFT), Main Boundry Thrust (MBT), Main Central Thrust (MCT), Ramgarh Thrust (RT).

variation displayed by the initial P-wave arrival across seismic stations positioned in distinct back azimuth relative to an earthquake. Specifically, the first motion can manifest as either compression, indicating movement towards the station, or dilatation, signifying movement away from it. The initial movement could be observed as compression, denoting an approach towards the station, or as dilatation, indicating a departure from it. Subsequently, upon arrival of a P wave at a seismograph station from beneath the Earth, the vertical component of the seismogram records an initial motion that is either rising or falling, representing compression or dilatation, respectively. The data necessary for determining the focal mechanism is gathered by collecting information on the first-arrival polarities and their azimuth from various recording stations. The process of establishing the solution for the focal mechanism using data on the first-arrival polarities needs a back-azimuthally distributed stations. In this study, eighteen events, as showing the data for representative catalogue in table 2, are selected with high-precision location parameters, a clear record of P-wave first motion polarity and a number of seismic stations.

Stress Tensor Inversion

Stress inversions of earthquake events were primarily conducted based on the distribution of FMSs, through which we get two sub-regions. For the stress inversion analysis 46 focal mechanisms, with magnitudes ranging from 3.2 to 8.7 were utilized. The construction of the database commenced with the collection of focal mechanisms derived from waveform modelling and the P-wave first polarity method, as documented in Pal *et al.* (2024b) along with ISC data (http://www.isc.ac.uk/isc-(ISC - EHB) data (ehb/) by Engdahl (1998) for an additional solution in the present study, culminating in the compilation of the earthquake focal mechanism database. Earthquake focal mechanism solutions were evaluated for the events recorded in the vicinity of Siang Antiform. Stress tensor analysis serves as a technique employed to examine the stress state in rocks by utilizing fault-slip data or earthquake focal mechanisms. This approach facilitates the comprehension of the tectonic evolution and deformation history of a specific area. The methodology for determining stress orientations was conducted following the Vavryčuk (2014) technique (STRESSINVERSE code), which builds upon the works of Michael (1984, 1987). His method is linear and iterative stress inversion and used in MATLAB environment. To deduce the regional stress tensor from earthquake FMSs (strike, dip, and rake) in the area, with the optimal stress tensors determined through stress inversion methodology. The current studies focus on delineating the alignment of the 3 primary stress axes, i.e. σ1, σ2, and σ3, with a hierarchical relationship of σ1 > σ2 > σ3. The assessment of stress attributes via focal mechanism inversion is based on the hypothesis of stress homogeneity across the source region, enabling the evaluation of the prevailing stress status within the study region. The methodology involves determining the optimal fit of regional principal stress orientations. The optimal stress tensor alignment can be determined (Gephart & Forsyth 1984) by assuming fault slip occurs along the direction of maximum resolved shear stress at the time of an earthquake (Bott 1959). The shape ratio R is characterized as the relationship between the intermediate stresses considered about the maximum and minimum horizontal stresses, thereby influencing the configuration of the stress ellipsoid. Therefore, we determined the orientations of the three principal stress directions σ1, σ2, and σ3, along with the shape ratio R, which characterizes the configuration of the stress ellipsoid as:

$$\sigma = \frac{\sigma 2 - \sigma 3}{\sigma 1 - \sigma 3}$$

All stress inversions are designed to determine the optimal stress tensor that corresponds to the provided focal mechanisms. This stress tensor is symmetric, which means it consists of only six independent components. The inversion technique introduced by Vavrycuk (2014) incorporates a

Table 2. *Computed parameters of focal mechanism solutions for the events used in the present study. NSS: Normal with Strike-Slip Fault, RSS: Reverse with strike-slip Fault, N: Normal Fault, SS: Strike-Slip fault, R: Reverse Fault.*

S. No.	Date (dd/mm/yyyy)	Time (h:m:s)	Latitude (°N)	Longitude (°E)	Depth (Km)	Magnitude (M_L)	Strike (°)	Dip (°)	Rake (°)	P-axis (°) Az.	P-axis (°) Pl.	T-axis (°) Az.	T-axis (°) Pl.	Type of fault
1	17/01/2019	04:47.6	28.62	94.84	28.9	3.5	218	52	-37	90.4	50.4	93.4	5.7	NSS
2	15/03/2019	30:20.5	28.9	95.2	30.7	3.5	240	33	42	183.9	19.6	58.7	58.2	RSS
3	02/07/2019	08:35.7	27.85	95.16	40.6	5.4	180	28	-89	267.5	72.9	89.2	17	N
4	14/07/2019	48:20.2	28.11	95.09	108.8	3.7	132	68	36	257.1	6.9	353.1	40.5	RSS
5	10/12/2019	16:51.3	28.23	95.53	32.8	3.6	85	68	55	199.9	15.7	312.2	53.3	RSS
6	02/02/2020	27:06.0	29.02	94.72	10	4.2	354	82	50	114.3	26	228	39.4	RSS
7	26/02/2020	50:17.2	28.42	95.1	9.2	3.7	60	60	90	150	15	330	75	R
8	18/03/2020	20:28.1	28.95	94.7	4.1	3.9	251	82	50	11.4	26	125	39.4	DSS
9	17/04/2020	23:03.5	28.48	95.22	15.2	3.5	240	62	-89	152.4	73	329.2	17	N
10	29/04/2020	41:51.9	28.91	94.77	10	3.8	180	60	-89	92.7	75	269.2	15	N
11	09/09/2020	42:48.0	28.58	95.2	9.8	3.8	252	70	-89	170	85	341.2	5	N
12	04/11/2020	21:57.1	28.53	95.25	3.2	3.5	240	71	30	8	6	102.1	34.3	SS
13	10/12/2020	29:52.5	28.42	94.8	48.6	3.5	240	66	-89	152	69	329.2	21	N
14	06/05/2021	38:42.5	28.7	94.91	42.6	4.6	65	54	37	9.4	4.1	274.6	49.4	SS
15	06/05/2021	10:14:53	28.54	94.76	32.5	4.3	255	80	35	22	16	122.2	31.4	SS
16	14/10/2021	36:27.1	28.54	95.02	21	4.4	96	78	-31	50.5	30.2	147.6	12	NSS
17	31/10/2021	38:07.3	28.44	94.98	36.3	4	276	77	-62	217.1	50.1	344.1	26.6	NSS
18	10/12/2021	03:29.5	28.87	95.04	37.8	4.3	188	52	-89	103.7	83	277.2	7	N

constraint for fault instability to differentiate actual fault slips from the provided data and to assess fault orientations; consequently, it requires multiple iteration steps. Throughout the iterations, the inversion evaluates the given auxiliary nodal planes, and utilizing the Mohr-Coulomb criterion, the identification of the true fault planes is conducted (Michael 1984; Zoback 2010; Vavryčuk 2014). It identifies the most unstable nodal plane as the true fault plane. This method of stress inversion can select the real fault plane based on the constraints of fault instability, thereby defines an optimal stress tensor. Typically, it requires 3 to 4 iterations. Initially, the inversion assesses the orientations of principal stresses and the shape ratio without any predefined fault planes, subsequently identifying the actual fault planes using the Mohr-Coulomb criterion. These processes are reiterated until the outcome aligns with the most accurate solution. The inversion results encompass a stereogram that illustrates P and T axes, a stereogram that depicts primary stress axes along with their precision, a graphical depiction of R values, and a visualization of Mohr circles (Figs. 3, 4 and 5). We investigated the tectonic style further using the stress regime index (R') values. The R' values come from shape ratios depending on which principal axes have the largest plunges. The aim of this investigation was to identify the dominant tectonic regime related with the seismic events in the area and ascertain the direction of the stress field in two specific zones located on the eastern and western limbs of the Siang antiform, where seismic activities are more prevalent in the western sector. Additionally, we combined the dataset from these two regions and identified the overall prevailing stress regime in Siang Valley and surrounding area in the EHS.

RESULTS AND DISCUSSIONS

Focal Mechanism Solutions

Table 2 lists the FMSs, and the plotted beach balls in figure 2a. In the Siang Valley and adjoining region, the FMSs primarily exhibit thrust mechanisms along with a combination of strike-slip mechanisms; the dipping planes oriented in the northeast exhibit similarities with the orientations of the primary tectonic faults and the subduction of the Indian plate. Despite this, the FMS of certain seismic events indicates extensional deformation within a compressional setting, implying a complex subsurface deformation pattern. In the eastern part of the Siang Antiform (Table 2, Fig. 2a), event no. 2 is located near the Lohit thrust, exhibiting a reverse with a strike-slip mechanism. Event no. 5 occurred north of the Pasighat thrust, also showing a reverse with a strike-slip mechanism, while event no. 9 is situated near the Bomdo thrust in the core of the Siang window, this event displays a low dipping normal fault mechanism with a focal depth of 15.2 kilometers. The source zone of the 1950 earthquake indicates a dextral strike-slip

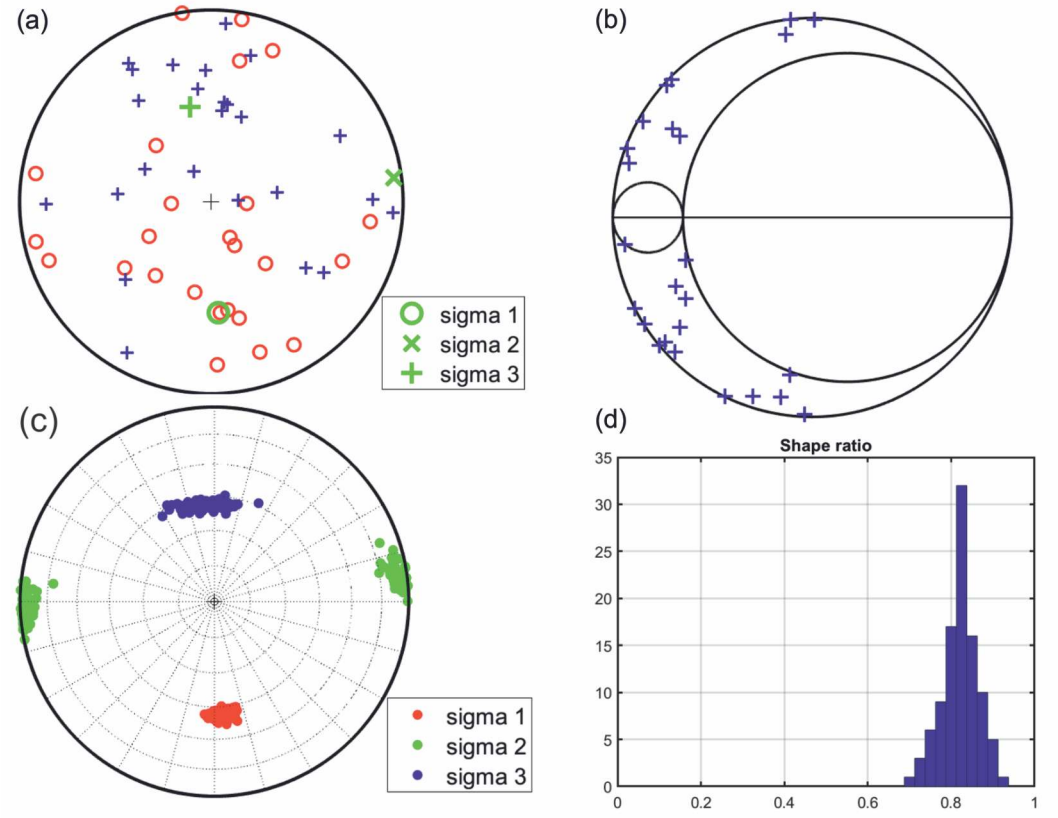


Fig. 3. Plot depicting outcomes of stress analysis performed in the western limb of Siang Window, (a) Plot showing P and T- axes with principal stress axes, the red circles marked the P- axes and T- axes by the blue cross; (b) Mohr's circles with position of fault instability (blue plus signs); (c) red, green, blue circles representing confidence limit of principle stresses sigma 1, 2, 3 direction, respectively; (d) histogram of shape ratio i.e. R.

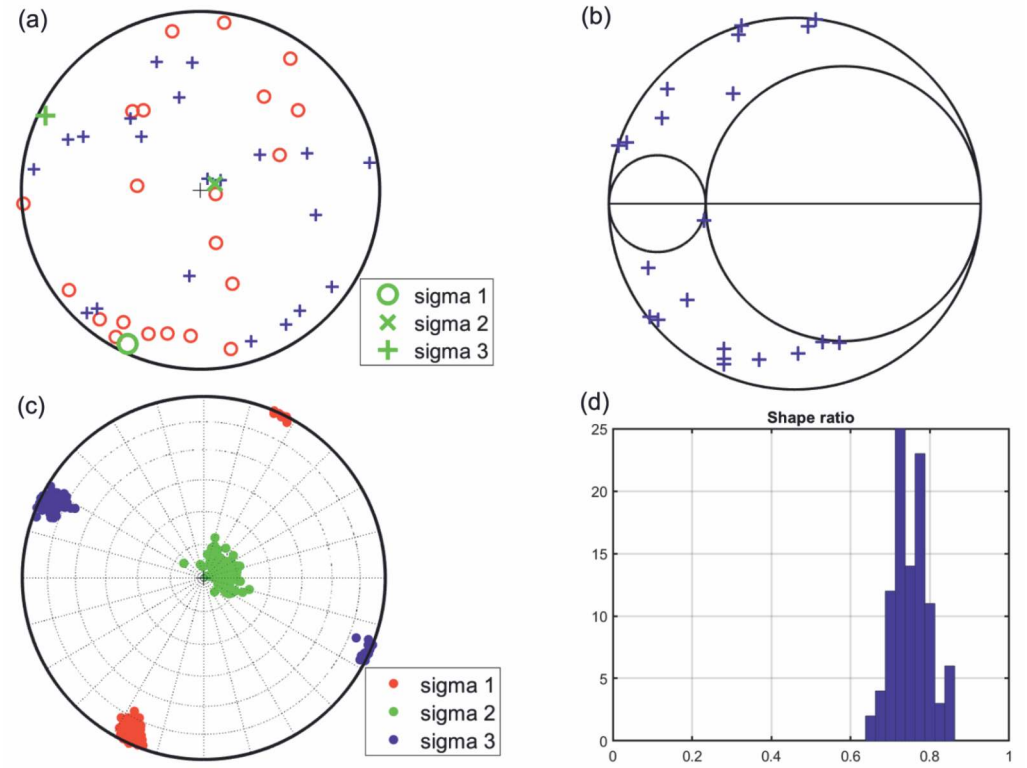


Fig. 4. Plot depicting outcomes of stress analysis performed in eastern limb of Siang Window, (a) Plot showing P and T- axes with principal stress axes, the red circles marked the P- axes and T- axes by the blue cross; (b) Mohr's circles with position of fault instability (blue plus signs); (c) red, green, blue circles representing confidence limit of principle stresses σ1, σ2 and σ3 direction, respectively; (d) histogram of shape ratio i.e. R.

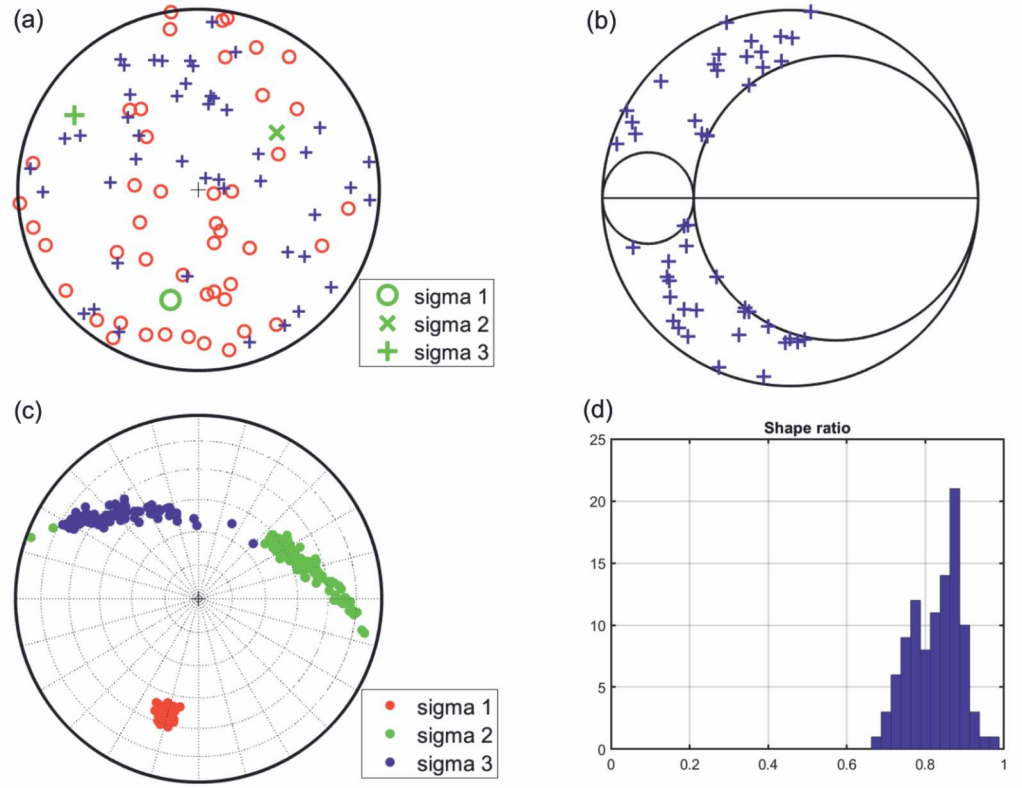


Fig. 5. Plot depicting outcomes of overall stress analysis performed in Siang Window, (a) Plot showing P- and T- axes with principal stress axes, the red circles marked the P- axes and T- axes by the blue cross; (b) Mohr's circles with position of fault instability (blue plus signs); (c) red, green, blue circles representing confidence limit of principle stresses sigma 1, 2, 3 direction, respectively; (d) histogram of shape ratio R.

movement of the plate to the north of the Lohit thrust on the eastern side of the Siang Valley (Ben-Menahem *et al.* 1974). Events no. 11 and 12 are close to each other and show dipping normal fault and strike-slip with reverse faulting, yet there is a significant difference in focal depth of 15.2 km and 3.2 km, respectively. Event no. 18 is comparatively deeper, showing normal faulting with a 37.8 km focal depth. The epicentre of Event no. 6 and 8 occurred north of the Siang antiform which shows reverse with strike slip mechanism with varying focal depth, while Event no. 10 shows low dipping normal faulting. The western part of the Siang window, which is more seismically active than the eastern part, has more number of earthquakes (events no. 1, 4, 7, 13, 15, 16 and 17, Table 2). Events no. 16 and 7 lie in the core of the Siang antiform, and show normal fault with strike slip and reverse fault mechanism while these epicentres are far away from each other. The deepper event 4 demonstrates a reverse with a strike slip fault mechanism. In contrast event number 17 exhibits a shallow focus normal with strike slip mechanism, both event (4 & 17) located on the Bomdo thrust with varying epicentre positions. Events 1 and 13 are situated along the Ramgarh thrust, displaying normal faulting at different focal depths. Event 15, along the MCT, displays a strike-slip mechanism up to a focal depth of 32.5 kilometers. Event 3, close to the MFT, showcases normal faulting. Chouhan & Srivastava (1975) analyzed the FMSs of seismic events in the northeastern region of India. Utilizing data on first-arrival polarities, they specifically focused on two-years. The findings of the study suggested the presence of strike slip faulting in the northern part and thrust type faulting in the southern part of the Myanmar ranges. According to Panthi *et al.* (2013), the dominant seismotectonic state in the Eastern Syntaxis regions displays a thrust mechanism, with instances of both normal and strike-slip faulting indicating compressional forces in the vicinity. Additionally, the present study results show that the main mechanism of energy release in the Eastern Himalayan region is mainly linked to thrust faulting, along with a combination of strike-slip mechanisms. The determination of the orientations of the P and T axes is derived from focal mechanism solutions (Table 2), facilitating the understanding of the stress distribution in the Siang Valley. By analyzing FMS, it is possible to ascertain the azimuth and dip angles of both the P- and T- axes.

Depth distribution of seismicity

The Northeastern Himalayan region exhibits a wide occurrence of seismic events ranging from moderate to high magnitude earthquakes within the crust (0-60 km depth). An identifiable grouping of seismic occurrences is specifically observed in the western part of Siang Antiform and Namche Barwa region. A detailed analysis of the depth distribution of earthquake epicentres has been carried out beneath this specific region by employing a north-south-oriented profile A-B (Fig. 2a & b) that divide the Siang Antiform into two sections and traverse through tectonic structures such as the Walong thrust, Lohit thrust, MCT, MBT, Bomdo thrust, Ramgarh Thrust, and the main frontal thrust. The depth distribution of earthquakes along section A-B is graphically represented with depth-projected FMSs along with major tectonic features and faults (Fig. 2b). The MCT, MBT, and MFT exhibit a dip in the northwest. Seismic activity is predominantly situated between the MFT and MBT within the depth section, while a noticeable cluster of earthquakes is evident in the upper crust extending up to a depth of 40 km. Earthquakes in the Eastern Himalayan region exhibit a high concentration within a specific area delineated by the MFT and MCT, thereby unveiling complex imbricate configuration in the frontal part of the Arunachal Himalaya. The frequency of earthquakes in the lesser Himalayan domain is closely tied to predominantly thrust motions along the MBT and MFT (Gupta *et al.* 2015). The spatial distribution of hypocenters at various depths aligns with previous research, indicating significant seismic activity in the western and eastern part of Siang Antiform, and Namche Barwa regions, respectively. Seismicity in the western portion of the Siang Valley is more pronounced in comparison to the other parts of the valley (Pal *et al.* 2024a). In the depth projection view (Fig. 2b), FMS close to the tectonic feature RT (event 10) shows strike-slip fault and near MBT, events 7, 9, 16 and 1 are normal and reverse with a combination of strike-slip mechanisms. Deeper earthquakes (events 5, 17, 14, 2 and 18) show thrust with strike-slip combination.

Stress Tensor Inversions Analysis

Stress Inversion is carried out on both the Western and Eastern sides of the Siang window in the Siang Valley, Arunachal Himalaya. The current stress distribution in this area is determined by utilizing focal mechanism data from these two distinct regions. In the process of inversion insights of significant value regarding the alignment of the primary axes of maximum compression (P), extension (T), and neutral (B) are elucidated through the utilization of inversion parameters. The outcomes derived from the inversion procedure, as depicted in figures 3, 4 & 5, encompass four distinct elements denoted as a, b, c, & d. These components exhibit the focal sphere that showcases the P and T axes, the optimal principal stresses, the Mohr circle, the stereographic projection portraying the principal stresses alongside their associated uncertainties, and a histogram that presents the shape ratios. The Mohr circle diagram's depiction helps to demonstrate the reliability of the results and the results of the stress inversion (Fig. 3b, 4b & 5b). Blue crosses were assigned to the possible orientations of fault slips (one slip direction belongs to each seismic event). If these crosses were located near the largest Mohr circle, that is between σ1 and σ3, their corresponding direction could be considered unstable and identified as that of the real fault plane. These solutions must be analyzed in relation to the P axes that are perpendicular to the dilatational quadrants. If the orientations of the σ1 and P axes align, then S_{hmax} vectors can be identified. Consequently, we can infer the type of tectonic regime that may be associated with the earthquakes.

In the western portion of the Siang Valley region, twenty-five focal mechanism solutions were utilized for the inversion, where three events, including the Mw 5.9 Mechuka Earthquake (Yadav *et al.* 2021), occurred along the MCT resulting in extensive surface ruptures. The primary alignment

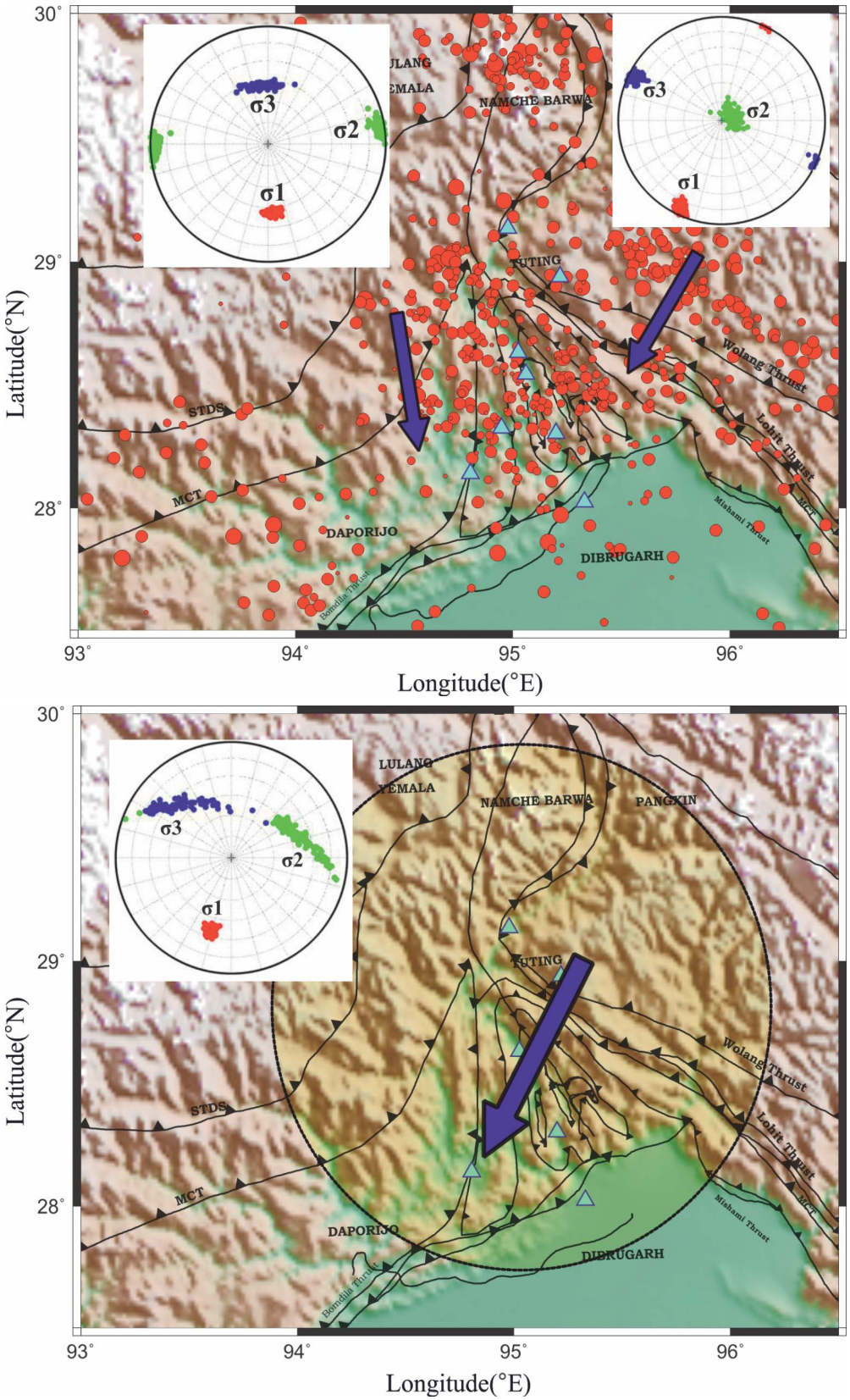


Fig. 6. (a) The plot depicts the FMS results of events used in the stress inversion analysis and the seismicity in and around Siang Valley. Cyan triangles represent the BBS station locations of recorded events. The maximum horizontal stress (Sh_{max}) direction in the western and eastern part of Siang Valley is SSE and SSW, respectively. (b) The direction of Sh_{max} in the Siang Valley of Arunachal Himalaya indicated by a Blue arrow, i.e. SSW.

of the maximum compression (P) axis is oriented towards the SSE direction (represented by red circles), with the azimuth of σ1 identified as N176.30 (approximately towards the South), illustrated in figure 3a, c. Upon utilizing the obtained inclinations of σ1 (red dots), σ2 (green dots), and σ3 (blue dots), the dominant tectonic regime is established. In the western portion of the Siang Valley region, the plunges of σ1, σ2, and σ3 measured approximately 41.6°, 4.5°, and 47.9°, respectively. These values suggest that the σ1 axis tends to be oriented nearer to the horizontal plane and the σ2 axis is horizontal, while the σ3 axis is near to the vertical, indicating a prevailing compressional stress regime within the area. A histogram depicting shape ratios has been developed based on the realizations (Fig. 3d). The peak observed in this histogram represents the optimal R-value, determined to be 0.82 for the western part of Siang Valley region. Through the assessment of the stress regime index (R'), incorporating the maximum plunge axes and R-value, valuable insights can be gained regarding the primary regional tectonic stress regime currently active in this geographical area (Delvaux *et al.* 1997; Czirok 2016). Three relations can be provided:

1. If σ1 is oriented vertically, the resultant R' equals R, demonstrating an extensional tectonic stress regime.
2. If σ2 is oriented vertically, the resultant R' equals 2 - R, suggesting a strike-slip or transverse tectonic stress regime.
3. If σ3 is oriented vertically, the resultant R' equals 2 + R, indicating a compressional tectonic stress regime.

Consequently, the value of R is ascertained with variations falling within the 0-3 range, indicating a radial extension at 0 to radial compression, at 3, tectonic conditions. Thus, R' equals 2.82, signifying the presence of a reverse type of faults and a radial compression tectonic setting. The determination of the predominant horizontal stress $S_{hmax's}$ orientation is dependent on the azimuth and plunge of the principal stress axes (Zoback 1992). The S_{hmax} azimuth in this area is calculated at 176.30°N (P-axes azimuth). Therefore, we conclude from here that earthquakes in the western part of Siang region are mostly exposed to thrust with strike-slip faulting, and the direction of S_{hmax} is towards almost south (Fig. 6a).

In the eastern part of the Siang Valley region, twenty-one fault plane solutions were used in the inversion process. The focal mechanism of the 1950 earthquake in Assam signifies the presence of a single strike-slip fault system, while subsequent seismic events suggest a combination of oblique motion-thrust faulting alongside a notable strike-slip component. In the eastern region, σ1 and σ3 exhibit nearly horizontal orientations, as indicated in Fig. 4c, with azimuths of 205.30° and 295.70°, respectively, while σ2 is positioned close to vertical. The calculated shape ratio values R (0.73) (Fig. 4d) and R' (1.27) propose the prevailing strike-slip tectonic regime in this area. The azimuth of the maximum horizontal stress, S_{hmax}, in this zone, is N 205.30°, corresponding to a south-southwest orientation (Fig. 6a).

We further amalgamated the moment tensors of the eastern and western sections of the Siang Valley region and conducted stress inversion analysis on the complete dataset. Our results (Fig. 5, Table 3) indicate that the σ1 (37.2°) and σ3 (20.8°) axes are oriented close to the horizontal, while the σ2 (45.4°) axis shows more proximity to the vertical position (with the highest plunge angle), suggesting a prevailing strike-slip regime within the Siang Valley area. The principal stress ratio (R) calculated for the integrated dataset equates to 0.75, whereas the R' value is determined to be 1.25. The combined dataset examination shows that the region is largely characterized by prominent strike-slip movements, with the primary stress direction σ1 pointing towards N194.30° (SSW), almost due south. The direction of S_{hmax} is SSW in this case (Fig. 6b). All the stress inversion parameters for the western, eastern and combined analysis of the study area are listed in Table 3. In contrast to the findings of Kamra *et al.* (2023), distinct patterns can be observed in the S_{hmax} values across different tectonic regions. Specifically, in the Shillong Plateau, a predominant northerly orientation indicates evident compressional forces. Conversely, the Mikir Hills display a northeast trend, suggesting a transtension regime. Moving to the eastern Himalayan zone, the S_{hmax} orientation shifts to SSW, indicating a prominent strike-slip regime and in the Indo-Burma zone, the S_{hmax} values align in a northeast direction, highlighting a clear compression regime.

CONCLUSIONS

The studies of FMS and stress inversion in seismically active regions of the Siang Valley within the EHS are conducted. This study was prompted by the occurrence of swarm earthquakes almost annually in the EHS locality. The spatial distribution of seismicity indicates groupings in the eastern and western parts of the Siang valley, as well as in the Namche Barwa vicinity within EHS, reaching depths of up to 60 km. The region of the Eastern Himalayas is primarily distinguished by the prevalence of reverse, strike-slip and a combination of both fault types. In the western sector of the Siang Valley, reverse faulting has a prevalence of with strike-slip characteristics. These faults are characterized by dip angles ranging from low to moderate. The data derived from the FMSs is utilized to gain insights into widespread contemporary tectonic regime in the area. In the NE Himalaya, stress tensor analysis has been applied to various structures, such as the MBT, MCT and Lohit thrust. The region is subdivided into two subareas, and forty-six fault plane solutions were used. It is found that the western side of the Siang Valley region shows radial compression; however, the eastern side shows a clear strike-slip regime. The azimuth of S_{hmax} is N176.3° on the western side and N205.3° on the eastern side. The inversion of the combined data set shows the clear strike-slip with maximum principal stress (σ1) oriented in N194.3°. The stress regime in the region is predominantly transverse, with a sub-horizontal maximum principal stress axis (σ1) oriented to SSW, consistent with the India-Eurasia plate convergence. The elevated seismicity observed in this area is attributed to the northward and eastward displacement of the Indian plate towards the Eurasian and Burmese plates, respectively.

Acknowledgements: The authors express their gratitude to the Director of the WIHG Dehradun for offering the necessary resources and support to carry out the research. We acknowledge Drs. Devajit Hazarika and Naresh Kumar, WIHG, for their assistance with the setup of the BBS stations and conducting fieldwork. The first author expresses gratitude to the University Grants Commission (UGC), New Delhi for providing financial assistance during the entire duration of the research.

Author Contributions: Ashish Pal (AP): Data curation, Data processing, investigation, methodology and writing-original draft. Dilip Kumar Yadav (DKY): conceptualization, validation and supervision. Debonil Baruah (DB): Visualization and editing. Abhishek Kumar Gupta (AKG): review and editing. H.C. Nainwal: supervision. Parakh Sahu (PS): Visualization

Data availability: Wave-form data could be acquired by sending a mail to the Director (director@wihg.res.in) WIHG, Dehradun, India.

Statements and Declarations: The authors assert that they do not have any documented conflicting financial benefits or own associations that may have impacted the research detailed in this investigation.

References

Acharya, S.K., Saha, P. 2013. Age and tectono-magmatic setting of abor volcanics, siang window, eastern himalayan syntaxial area, India. *Journal of Applied Geochemistry*, **15**(2), 170-192.

Baruah, S., Duarah, R., Yadav, D.K. 1997. Pattern of Seismicity in Shillong-Mikir Plateau and the orientation of compressional axis. *Journal Geological Society of India*, **49**(5), 533-538.

Ben-Menahem, A., Aboodi, E., Schild, R. 1974. The source of the great Assam earthquake—an interplate wedge motion. *Physics of the Earth and Planetary Interiors,* **9**(4), 265-89.

Bilham, R., England, P. 2001. Plateau "Pop-Up" in the Great 1897 Assam Earthquake. Nature, 410, 806-809. https://doi.org/10.1038/35071057

Bilham, R. 2006. Comment on "Interpreting the style of faulting and paleoseismicity associated with the 1897 Shillong, northeast India, earthquake" by C. P. Rajendran et al. *Tectonics*, 25 (2). doi:10.1029/2005tc001893

Bott, M.H.P. 1959. The Mechanics of Oblique Slip Faulting. *Geological Magazine,* 96, 109-117. https://doi.org/10.1017/S0016756800059987

Chandra, U. 1978. Seismicity, Earthquake Mechanisms and Tectonics along the Himalayan Mountain Range and Vicinity, *Physics of the Earth and Planetary Interiors*, 16, 109-131. https://doi.org/10.1016/0031-9201(78)90083-3

Chen, W.P., and Molnar, P. 1990. "Source Parameters of Earthquakes and Intraplate Deformation beneath the Shillong Plateau and the Northern Indo-Burman Range," *Journal of Geophysical Research*, Vol. 95, No. B8, 12527-12552. doi:10.1029/JB095iB08p12527

Chouhan, R.K.S., Srivastava, V.K.1975. Focal mechanisms in northeastern India and their tectonic implications. *PAGEOPH* **113**, 467-482. https://doi.org/10.1007/BF01592932.

Curray, J.R., Emmel, F.J., Moore, D.G., Raitt, R.W. 1982. Structure, Tectonics, and Geological History of the Northeastern Indian Ocean. In: Nairn, A.E.M., Stehli, F.G. (eds) The Ocean Basins and Margins. Springer, Boston, 399-450. https://doi.org/10.1007/978-1-4615-8038-6_9.

Czirok, L. 2016. Analysis of stress relations using focal mechanism solutions in the Pannonian basin. *Geosciences and Engineering: a Publication of the University of Miskolc*, **5**(8), 65-84.

Delvaux, D., Moeys, R., Stapel, G., Petit, C., Levi, K., Miroshnichenko, A., Ruzhich, V., San'kov, V. 1997. Paleostress reconstructions and geodynamics of the Baikal region, central Asia, Part 2. Cenozoic rifting. *Tectonophysics*, **282**(1-4), 1-38.

Engdahl, E.R., van der Hilst, R., Buland, R. 1998. Global teleseismic earthquake relocation with improved travel times and procedures for depth determination, *Bulletin of the Seismological Society of America*, **88**, 722-743.

Gephart, J.W., Forsyth, D.W. 1984. An improved method for determining the regional stress tensor using earthquake focal mechanism data: application to the San Fernando earthquake sequence. *Journal of Geophysical Research: Solid Earth*, **89**(B11), 9305-9320.

Gupta, S.D., Nandy, D.R. 1982. Seismicity and Tectonics of Meghalaya Plateau, Northeastern India. VII Symposium on Earthquake Engineering, University of Roorkee, Roorkee, India, Vol.: I, (19-24).

Gupta, H.K., Singh, S.C., Dutta, T.K. & Saikia, M.M. 1984. Recent investigations of North East India seismicity. *In:* Gongu, G., Xing-Yuan, M. (eds.), Proceedings of the Interna-tional Symposium on Continental Seismicity and Earthquake Prediction, pp. 63-71. Seismological Press, Beijing.

Gupta, T.D., Riguzzi, F., Dasgupta, S., Mukhopadhyay, B., Roy, S., Sharma, S. 2015. Kinematics and strain rates of the Eastern Himalayan Syntaxis from new GPS campaigns in Northeast India. *Tectonophysics*, **655**, 15-26. 10.1016/j.tecto.2015.04.017

Gururajan, N.S., Choudhuri, B.K. 2003. Geology and tectonic history of the Lohit Valley, Eastern Arunachal Pradesh, India. *Journal of Asian Earth Sciences*, **21**(7), 731-741.

Havskov, J., Ottemoller, L. 1999. SEISAN earthquake analysis software. *Seismological Research Letters*, **70**(5), 532-534.

Hazarika, D., Kundu, A., Ghosh, P. 2022. Seismotectonic scenario of the indenting northeast corner of the Indian plate in the Tidding-Tuting Suture Zone of the Eastern Himalayan Syntaxis. *Tectonophysics*, **824**, 229197. https://doi.org/10.1016/j.tecto.2021.229197

Kamra, C., Chopra, S., Yadav, R.B.S. 2023. Tectonic stress of northeastern Indian region derived from seismic focal mechanisms and the effect of focal mechanism on stress drop: a comparative analysis with Kachchh intraplate region of India. *Geophysical Journal International*, **234**(1), 453-478.

Kayal, J.R. 1991. Earthquake prediction in Northeast India-a review. *Pure and applied Geophysics*, **136**, 297-313.

Kayal, J.R. 1998. Seismicity of Northeast India and surrounding-development over the past 100 years. *Journal of Geophysics*, **29**(1), 9-34.

Kayal, J.R., De, R. 1991. Microseismicity and tectonics in northeast India. *Bulletin of the Seismological Society of America*, **81**(1), 131-138.

Kayal, J.R., Arefiev, S.S., Barua, S., Hazarika, D., Gogoi, N., Kumar, A., Chowdhury, S.N., Kalita, S. 2006. "Shillong Plateau Earthquakes in Northeast India Region: Complex Tectonic Model. *Current Science*, **19**, 109-114.

Khattri, K.M., Tyagi, A.K. 1983. Seismicity patterns in the Himalayan plate boundary and identification of the areas of high seismic potential. *Tectonophysics*, **96**(3-4), 281-297.

Le Fort, P. 1975. Himalayas: the collided range. Present knowledge of the continental arc. *American Journal of Science*, **275A**, 1-44.

Lee, W.H., Lahr, J.C. 1975. HYPO71 (revised; a computer program for determining hypocenter, magnitude, and first motion pattern of local earthquakes. *Open-File Report* Vol. 1975 (75-311) US Geological Survey. doi:10.3133/ofr75311

Michael, A.J. 1984. Determination of stress from slip data: faults and folds. *Journal of Geophysical Research: Solid Earth*, **89**(B13), 11517-11526.

Michael, A.J. 1987. Use of focal mechanisms to determine stress: a control study. *Journal of Geophysical Research: Solid Earth*, **92**(B1), 357-368.

Mitchell, A.H.G. 1981. Phanerozoic plate boundaries in mainland SE Asia, the Himalaya and Tibet. *Journal of Geological Society of London*, **138**, 109-122.

Mitra, S., Priestley, K., Bhattacharyya, A., Gaur, V.K. 2005. Crustal structure and earthquake focal depths beneath northeastern India and southern Tibet. *Geophysical Journal International*, **160**, 227-248.

Molnar, P., Tapponnier, P. 1975. Cenozoic Tectonics of Asia: Effects of a Continental Collision: Features of recent continental tectonics in Asia can be interpreted as results of the India-Eurasia collision. *Science*, **189**(4201), 419-426.

Nandy, D.R. 2001. *Geodynamics of Northeastern India and Adjoining Region*. ABC Publ., Kolkata, India, 209p.

Ni, J., Barazangi, M. 1984. Seismotectonics of the Himalayan collision zone: Geometry of the underthrusting Indian plate beneath the Himalaya. *Journal of Geophysical Research: Solid Earth*, **89**(B2), 1147-1163.

Pal, A., Yadav, D.K., Kumar, N., Gupta, A.K., Paul, A., Nainwal, H.C. 2024a. Modelling of source parameters of local earthquakes and seismotectonic implications in Siang Valley, NE India. *Journal of Earth System Science*, **133**(2), 63. https://doi.org/10.1007/s12040-024-02272-9

Pal, A., Yadav, D.K., Gupta, A. K., Nainwal, H.C. 2024b. Seismotectonics of Siang Valley and Adjoining Region Inferred from Focal Mechanism Solutions Using Waveform Inversion. *Pure Appl. Geophys.* https://doi.org/10.1007/s00024-024-03518-9

Panthi, A., Singh, H.N., Shanker, D. 2013. Revisiting state of stress and geodynamic processes in Northeast India Himalaya and its adjoining region. *Geosciences*, **3**(5), 143-152.

Priestley, K., Jackson, J., McKenzie, D. 2008. Lithospheric structure and deep earthquakes beneath India, the Himalaya and southern Tibet. *Geophysical Journal International*, **172**(1), 345-362.

Poddar, M.C. 1950. The Assam earthquake of 15th August 1950. *Indian Minerals*. **4**, 167-176.

Raoof, J., Mukhopadhyay, S., Koulakov, I., Kayal, J.R. 2017. 3-D seismic tomography of the lithosphere and its geodynamic implications beneath the northeast India region. *Tectonics*, **36**(5), 962-980.

Rai, A., Mittal, H., Singh, G.P. 2024. Estimation of source and spectral decay parameter for local earthquake in the Siang region of Arunachal Himalya and its Implication to the Tectonic and crustal heterogeneity. *Pure and Applied Geophysics*, **181**, 789-813.

Rajendran, C.P., Rajendran, K., Duarah, B.P., Baruah, S., Earnest, A. 2004. Interpreting the style of faulting and paleoseismicity associated with the 1897 Shillong, northeast India, Earthquake: implications for regional tectonism. *Tectonics*, **23**, TC4009. doi:10.1029/2003TC001605, 2004

Rastogi, B.K., Singh, J., Verma, R.K. 1973. Earthquake mechanisms and tectonics in the Assam-Burma region. *Tectonophysics*, **18**(3-4), 355-366.

Salvi, D., Mathew, G., Pande, K., Kohn, B.P. 2021. Phased cooling of the Siang antiform, Eastern Himalaya: Insight from multi-thermochronology and thermal studies. *Journal of Earth System Science,* **130**, 1-20.

Singh, S. 1993. Geology and tectonics of the eastern syntaxial bend, Arunachal Himalaya. *Journal of Himalayan Geology,* **4**, 149-163.

Snoke, J.A., Munsey, J.W., Teague, A.G. , Bollinger, G.A. 1984. A Program for Focal Mechanism Determination by Combined Use of Polarity and SV-P Amplitude Ratio Data. *Earthquake Notes*, 55, 15.

Snoke, J.A., Lee, W.H.K., Kanamori, H., Jennings, P.C., Kisslinger, C. 2003. FOCMEC: Focal mechanism determinations. *International handbook of earthquake and engineering seismology*, **85**, 1629-1630.

Tapponnier, P., Pelzer, G., Ledain, A.Y., Armijo, R., Cobbold P. 1982. Prop agating extrusion tectonics in Asia: new insights from simple experiments with plasticine. *Geology*, **10**, 611-616.

Tapponnier, P., Peltzer, G., Armijo, R. 1986. On the mechanics of the collision between India and Asia. *Geological Society, London, Special Publications*, **19**(1), 113-157.

Thingbaijam, K.K.S., Nath, S.K., Yadav, A., Raj, A., Walling, M.Y., Mohanty, W.K. 2008. Recent seismicity in Northeast India and its adjoining region. *Journal of Seismology*, **12**, 107-123.

Valdiya, K.S. 1980. The two intracrustal boundary thrusts of the Himalaya. *Tectonophysics*, **66**(4), 323-348.

Vavryčuk, V. 2014. Iterative joint inversion for stress and fault orientations from focal mechanisms. *Geophysical Journal International*, **199**(1), 69-77.

Yadav, D.K., Hazarika, D., Kumar, N., Singh, A.K. 2021. Microseismicity study in the Siang Valley of Arunachal Himalaya: tectonic Implications of the 2019 Mw 5.9 Mechuka earthquake. *Himalayan Geology*, **42**(2), 290-298.

Yang, R., Herman, F., Fellin, M.G., Maden, C. 2018. Exhumation and topographic evolution of the Namche Barwa Syntaxis, eastern Himalaya. *Tectonophysics*, **722**, 43-52.

Zhao, W., Nelson, K.D., Che, J., Quo, J., Lu, D., Wu, C., Liu, X. 1993. Deep seismic reflection evidence for continental underthrusting beneath southern Tibet. *Nature*, **366**(6455), 557-559.

Zoback, M.D. 2010. *Reservoir Geomechanics*. Cambridge university press. https://doi.org/10.1017/CBO9780511586477

Zoback, M.L. 1992. First-and second-order patterns of stress in the lithosphere: The World Stress Map Project. *Journal of Geophysical Research: Solid Earth*, **97**(B8), 11703-11728.